Hydrothermal alteration can result in pore pressurization and volcano instability

Michael Heap, Tobias Baumann, H. Albert Gilg, Stephan Kolzenburg, Amy Ryan, Marlène Villeneuve, J. Kelly Russell, Lori Kennedy, Marina Rosas-Carbajal, Michael Clynne

Hydrothermal alteration can result in pore pressurization and volcano instability

Michael J. Heap[1], Tobias Baumann[2], H. Albert Gilg[3], Stephan Kolzenburg[4], Amy G. Ryan[5,6], Marlène Villeneuve[7], J. Kelly Russell[6], Lori A. Kennedy[6], Marina Rosas-Carbajal[8], and Michael A. Clynne[9]

[1] Université de Strasbourg, CNRS, Institut Terre et Environnement de Strasbourg, UMR 7063, 5 rue René Descartes, Strasbourg 67084, France

[2] Institute of Geosciences, Johannes Gutenberg University Mainz, J.-J.-Becher-Weg 21 D-55128, Germany

[3] Technical University of Munich, Arcisstr. 21 Munich, 80333 Germany

[4] Department of Geology, University of Buffalo, NY 14260-4130, USA

[5] Department of Earth and Environmental Sciences, University of Minnesota, MN 55455, USA

[6] Department of Earth, Ocean and Atmospheric Sciences, University of British Columbia, British Columbia V6T 1Z4, Canada

[7] Montanuniversität Leoben, Erzherzog Johann-Straße 3, Leoben A-8700, Austria

[8] Institut de Physique du Globe de Paris, 1 Rue Jussieu, Paris 75005, France

[9] U.S. Geological Survey, Volcano Science Center, Menlo Park, CA 94025, USA

ABSTRACT

The collapse of a volcanic flank can have dire consequences. Hydrothermal alteration is common to volcanoes worldwide and is thought to promote volcano instability by decreasing rock strength. However, some laboratory studies have shown that not all alteration reduces rock

strength. Our new laboratory data for altered rhyodacites from Chaos Crags (Lassen Volcanic Center, USA) show that pore- and crack-filling mineral precipitation can reduce porosity and permeability and increase strength, Young's modulus, and cohesion. A significant reduction in permeability, by as much as four orders of magnitude, will inhibit fluid circulation and create zones of high pore fluid pressure. Here we explore the consequences of pore fluid pressurization on volcano stability using large-scale numerical modeling. Upscaled physical and mechanical properties for hydrothermally altered rocks are used as input parameters in our modeling. We show that a high pore pressure zone within a volcano increases volcano deformation and that increasing the size of this zone increases the observed deformation. Hydrothermal alteration associated with mineral precipitation, and increases to rock strength, can therefore promote pore pressurization and volcano deformation, increasing the likelihood of volcano spreading, flank collapses, and phreatic/phreatomagmatic explosions. We conclude that porosity-decreasing alteration, explored here, and porosity-increasing alteration can both promote volcano instability and collapse, but by different mechanisms. Hydrothermal alteration should therefore be monitored at volcanoes worldwide and incorporated into hazard assessments.

INTRODUCTION

Volcanoes are inherently unstable structures and mass wasting events, sometimes destructive and deadly, are commonplace. As a result, volcano stability assessments are performed at volcanoes worldwide and the mechanisms thought to influence volcano stability have been studied and debated at length. Hydrothermal alteration resulting from the circulation of hot, magmatic fluids is often considered to reduce rock strength and promote volcano instability (López and Williams, 1993; van Wyk de Vries et al., 2000; Reid et al., 2001; John et al., 2008; Rosas-

Carbajal et al., 2016). However, experimental studies suggest that alteration type dictates whether volcanic rock will weaken or strengthen (Wyering et al., 2014; Frolova et al., 2014). Alteration associated with porosity reduction and/or the formation of clays reduces strength (Potro and Hürlimann, 2009; Farquharson et al., 2019); conversely, alteration that decreases porosity increases strength (Mordensky et al., 2018; Heap et al., 2020a). Given the relationship between porosity and strength (Heap and Violay, 2021), alteration could be expected to either enhance or reduce volcano stability, depending on the alteration type. However, permeability is also greatly reduced by porosity-filling alteration (Mordensky et al., 2018; Heap et al., 2019) which can inhibit fluid circulation and promote pore fluid pressurization within the volcano, a phenomenon considered to facilitate volcano instability and collapse (Day, 1996; Reid, 2004; Ball et al., 2018). For example, the modeling of Ball et al. (2018) showed that water saturation and elevated pore pressure can decrease volcano stability and increase collapse volume. As noted by Ball et al. (2018), the scarcity of petrophysical properties for altered volcanic rocks limits the investigation of volcano stability using large-scale models.

Here we combine upscaled laboratory data for variably altered volcanic rocks with large-scale numerical modeling to explore the influence of hydrothermal alteration on volcanic stability. We show that alteration resulting in an increase in rock strength can promote pore pressurization and volcano deformation, increasing the likelihood of volcano spreading, flank collapses, and phreatic/phreatomagmatic explosions. We conclude that porosity-decreasing alteration, explored here, and porosity-increasing alteration can both promote volcano instability, but by different mechanisms.

MATERIALS AND METHODS

Four blocks were collected from Dome C at Chaos Crags (Lassen Volcanic Center, USA; Fig. 1A). The majority of Dome C collapsed ~350 years ago (Clynne and Muffler, 2017), leaving a semi-spherical collapse scar and an avalanche deposit called Chaos Jumbles (Fig. 1A). We sampled one block from the Chaos Jumbles deposit, considered to represent largely unaltered dome material (sample CCC), and three visibly-altered blocks (CC4A, CC4B, and CC10) collected from the altered carapace of the dome that now forms the collapse scar.

All blocks are porphyritic rhyodacitic dome lavas that contain phenocrysts within a crystallized groundmass (backscattered scanning electron microscope (SEM) images are provided in the Data Repository). The mineral content of the four blocks was quantified using X-ray powder diffraction (see Data Repository). The unaltered dome material (CCC) contains plagioclase (52.6 wt.%), K-feldspar (16.8 wt.%), and quartz (17.8 wt.%) with minor quantities (<10 wt.%) of cristobalite, biotite, hornblende, clinopyroxene, magnetite, and hematite. The mineral contents of samples CC4A and CC4B are similar to CCC, but contain more cristobalite and additional smectite (0.9–1.3 wt.%) and kaolinite (4.2–4.8 wt.%) (i.e. intermediate argillic alteration). Sample CC10 has similar quantities of plagioclase as CCC, but less K-feldspar and quartz and more cristobalite.

Rock physical and mechanical properties were measured to characterize each block and to provide input parameters for the large-scale modeling. Cylindrical samples, 20 mm in diameter and 40 mm in length, were prepared from each of the blocks. Connected porosity was calculated using the bulk sample volume and the skeletal sample volume measured by a helium pycnometer. Permeability was measured using a gas permeameter (Heap and Kennedy, 2016) under a confining pressure of 1 MPa. Uniaxial compressive strength experiments were performed on select oven-dry samples of each of the blocks using a constant axial strain rate of 10^{-5} s^{-1}. The static Young's modulus was determined from the elastic portion of the uniaxial stress-strain curves. Triaxial

compression experiments were performed on water-saturated samples of the least (sample CCC) and most altered (sample CC4A, the sample that contains the highest wt.% of alteration minerals) blocks using a pore fluid (water) pressure of 10 MPa, confining pressures between 12.5 and 30 MPa, and a constant axial strain rate of 10^{-5} s^{-1}.

INFLUENCE OF ALTERATION ON ROCK PROPERTIES

Permeability is plotted as a function of connected porosity in Fig. 1B (plots of Young's modulus and uniaxial compressive strength as a function of connected porosity are provided in the Data Repository). The permeability of the unaltered dome material (CCC) is consistently ~10^{-14} m^2. Although the permeability of altered block CC10 is also ~10^{-14} m^2, the permeability of altered blocks CC4A and CC4B vary from ~10^{-18} to ~10^{-17} m^2 and from ~10^{-16} to ~10^{-14} m^2, respectively (Fig. 1B). The decrease in porosity and permeability as a result of increasing alteration is indicated by the black arrow (Fig. 1B). The Young's modulus and uniaxial compressive strength of blocks CCC, CC4B, and CC10 are ~7–10 GPa and ~40–55 MPa, respectively. Altered block CC4A, however, has a much higher Young's modulus of ~30–35 GPa and a uniaxial compressive strength of ~120–140 MPa (data are available in the Data Repository). The triaxial deformation experiments show that the strength of the unaltered (sample CCC) and altered (CC4A) blocks increase as a function of increasing effective pressure (stress-strain curves are provided in the Data Repository). The laboratory-scale cohesion and angle of internal friction, calculated using these triaxial data, are 9 MPa and 54° and 16 MPa and 49° for blocks CCC and CC4A, respectively. In summary, hydrothermal alteration decreased the porosity and permeability and increased the strength, Young's modulus, and cohesion.

Experimental studies have shown that porosity-filling alteration can greatly reduce permeability (Mordensky et al., 2018; Heap et al., 2019; Kennedy et al., 2020) and increase strength (Wyering et al., 2014; Mordensky et al., 2018; Heap et al., 2020a), highlighting that the observed alteration-induced permeability reduction is not restricted to the rhyodacites measured here. Heap et al. (2019) showed that porosity-filling alunite group minerals reduced the permeability of basaltic-andesites from Merapi volcano (Indonesia) by up to four orders of magnitude. Mordensky et al. (2018) found that porosity-filling clay precipitation (smectite and kaolinite) increased the strength of andesites from Ruapehu (New Zealand). SEM images of block CC4A, the block with the lowest permeability, show that pores and cracks are filled with early cristobalite and late colloform hematite and kaolinite (Fig. 1C; Data Repository). Therefore, we conclude that the lower porosity and permeability and the higher strength, Young's modulus, and cohesion of CC4A, compared to the relatively unaltered sample (CCC), is the result of porosity-filling mineral precipitation.

INFLUENCE OF PORE PRESSURIZATION ON VOLCANO STABILITY

We use numerical modeling to demonstrate the potential influence of high pore pressure zones on volcano stability. We use the hydro-thermo-mechanical modeling code LaMEM (Lithosphere and Mantle Evolution Model; Kaus et al., 2016; described in detail in the Data Repository), which models the non-linear, visco-elastoplastic deformation of rocks and uses the Drucker-Prager failure criterion to constrain plastic strain rates. Numerically, LaMEM uses a staggered-grid finite difference method for discretization and a marker-and-cell method to assign and track rock properties within a Eulerian advection framework (Harlow and Welch, 1965).

Models were run on simplified 2D cross-sections of an idealized volcano, with a height of 2000 m, a slope angle of 30°, and a numerical grid of 4 × 3 m, built using the geomIO tool (Bauville and Baumann, 2019). The triangle-shaped volcano structure with volcanic dome (see thumbnail in Fig. 2A) is deformable and the sides and top of the volcano are free surfaces. The area beneath this structure is non-deformable and a free-slip boundary separates the two domains (i.e. we assume that the edifice rocks are weaker than the basement rocks). Additional models with no-slip boundary (edifice rocks have a similar strength to those of the basement) are provided in the Data Repository. By modifying the segmentation of the deformable domain, we prepared cross-sections for (1) a homogeneous volcano with no high pore pressure zone (thumbnail in Fig. 2A) and (2) volcanoes featuring high pore pressure zones of different sizes (thumbnails in Fig. 2B-D). Zones within the volcano cross-sections were designated as either unaltered (light and dark gray zones) or altered (yellow zones). Upscaled mechanical properties of samples CCC and CC4A were assigned to the unaltered and altered zones, respectively (Table 1; upscaling methods are described in detail in the Data Repository). Based on the results of Ball et al. (2018), which show that an order of magnitude decrease in permeability can increase pore pressure by a factor 2–4, we doubled the pore pressure ratio, λ_i, in the altered zone to account for its low permeability (Fig. 1B). We assume that the volcano is entirely fluid saturated, and that $p_f = p_h + \lambda_i (p_{lith} - p_h)$, where p_f, p_h, and p_{lith} are the pore fluid, hydrostatic, and lithostatic pressure, respectively.

Fig. 2 shows the total displacement field and displacement vectors after 500 years for each of the four modeled scenarios. Our modeling shows, for scenarios when alteration decreases porosity and permeability, that the presence of a high pore pressure zone within the volcano greatly increases volcano deformation and that increasing the size of the high pore pressure zone exacerbates the deformation (Fig. 2). The modeled deformation of the volcano consists of the

downward movement of the high central portion of the volcano and the lateral spreading of the flanks (Fig. 2), consistent with the analog modeling of Cecchi et al. (2004). Volcano spreading, promoted here by alteration and high pore pressure zones, is understood to initiate catastrophic flank collapses (van Wyk de Vries and Francis, 1997). Our modeling therefore suggests that high pore pressure zones, the result of porosity-decreasing alteration, can create a "critical state volcano" that is prone to volcano spreading and partial flank collapse, but also hydrofracturing/tuffisite formation and phreatic and phreatomagmatic explosions (Fig. 3). Ancillary models using the no-slip boundary condition show that deformation is more concentrated on the flanks, and that the maximum displacement is reduced (Data Repository).

Our modeling assumes that high pore pressures are maintained in the altered zone. We highlight that both volcano deformation and high pore fluid pressures can result in fracturing, which can decrease pore pressure. We envisage a scenario, similar to that described in Kennedy et al. (2020), in which fractures are eventually sealed by hydrothermal minerals within the alteration zone, allowing pore pressure to re-increase (i.e. long-term high pore pressure is punctuated by transient pore pressure reductions).

CONCLUDING REMARKS

Our large-scale numerical modeling, used in conjunction with well-constrained physical and mechanical property input parameters for hydrothermally altered rock, shows that high pore pressure zones promote volcano instability and collapse. High pressure zones in volcanoes can result from porosity reduction attending hydrothermal alteration. Thus, volcano stability can be undermined by alteration that results in either an increase or decrease in porosity, but by different mechanisms. Previous studies have shown that increasing porosity lowers the strength, Young's

modulus, and cohesion of volcanic rock, leading to a reduction in rock mass stability (Apuani et al., 2005). Although decreasing the porosity increases strength, we show here that it also significantly decreases permeability (Fig. 1B) and allows high pore pressure zones to develop that create a "critical state volcano" that is prone to not only volcano spreading and partial flank collapse, but also hydrofracturing/tuffisite formation and phreatic and phreatomagmatic explosions (Fig. 3). Since most volcanoes likely contain zones characterized by both of these different alteration styles, both mechanisms likely work in tandem to promote volcano instability. Therefore, it is important to monitor the extent and evolution of hydrothermal alteration zones using methods such as geological mapping (van Wyk de Vries et al., 2000), deformation monitoring (Moretti et al., 2020), muon (Rosas-Carbajal et al., 2017) and electrical tomography (Rosas-Carbajal et al., 2016), gas monitoring (de Moor et al., 2019), magnetic methods (Finn et al., 2007), and spectroscopic methods (John et al., 2008; Kereszturi et al., 2020). However, we also show that it is of equal importance to know the locations within the volcano prone to porosity-increasing (e.g., dissolution) and porosity-decreasing (e.g., precipitation) alteration styles, which will depend on factors such as pressure, temperature, and the pH and composition of the hydrothermal fluids.

ACKNOWLEDGMENTS

We thank M. Harris, B. Renaudié, T. Reuschlé, the United States National Park Service (LAVO-00050; LAVO-2019-SCI-0010), and the Canadian NSERC Discovery Grants program (RGPIN-2018-03841). Any use of trade, firm, or product names is for descriptive purposes only and does not imply endorsement by the U.S. Government.

205 **FIGURE CAPTIONS**

206

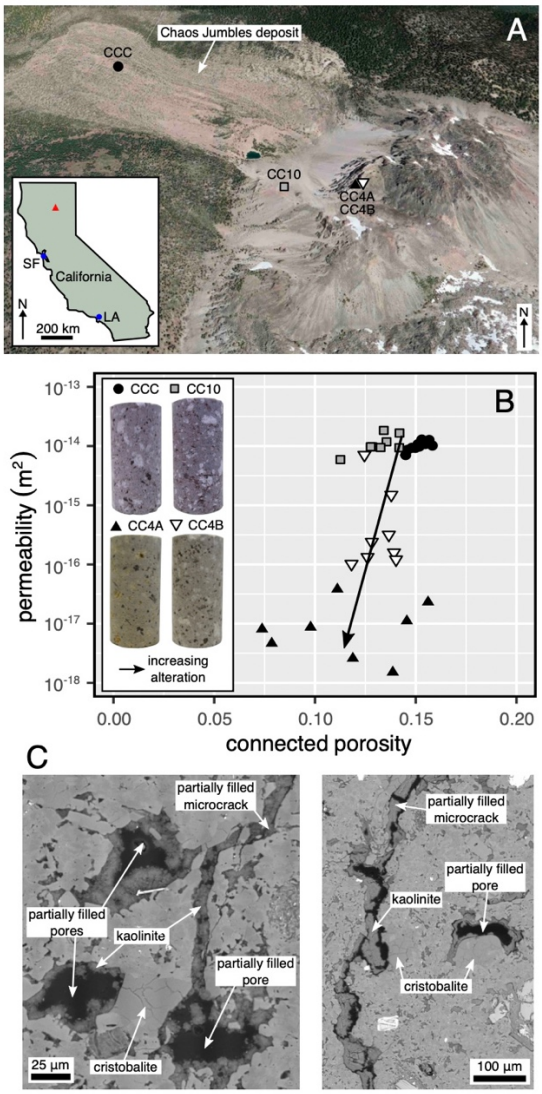

207

208 **Fig. 1.** A: Google Earth® image of Chaos Crags showing the sampling sites. Inset shows the
209 location of Chaos Crags (red triangle) in California (USA). SF – San Francisco; LA – Los Angeles.
210 B: Permeability as a function of connected porosity for the four blocks collected. Inset shows
211 photographs of the 20 mm-diameter samples. The black arrow indicates the increasing degree of
212 alteration. C: Backscattered scanning electron microscope images of sample CC4A showing
213 porosity-filling alteration.

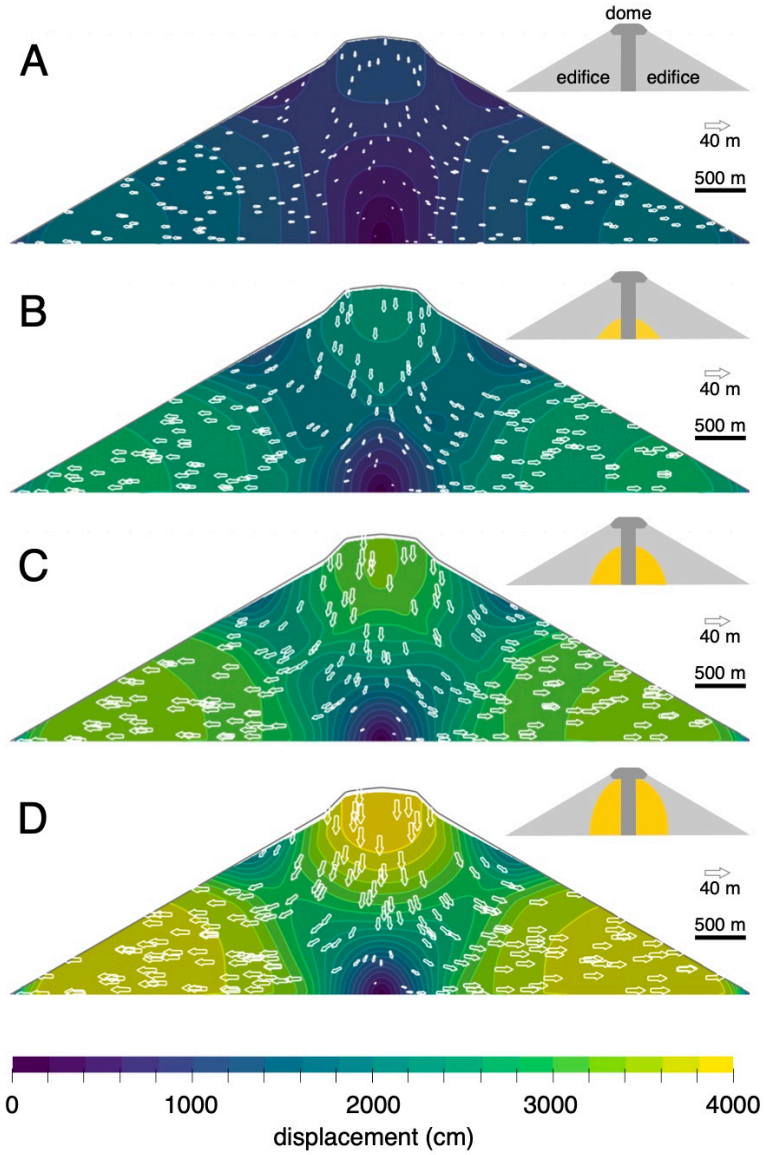

214

215 **Fig. 2.** Results of the large-scale volcano stability modeling. Colors indicate the total displacement
216 field (blue and yellow colors indicate low and high displacement, respectively) and the white
217 arrows show the displacement vectors. Models were run for 500 years. Thumbnails show the
218 model setup, where gray and yellow zones are unaltered and altered zones with a high pore
219 pressure, respectively (see Table 1 for model input parameters). A: Homogeneous volcano. B:
220 Volcano with a small alteration zone. C: Volcano with the medium alteration zone. D: Volcano
221 with a large alteration zone.

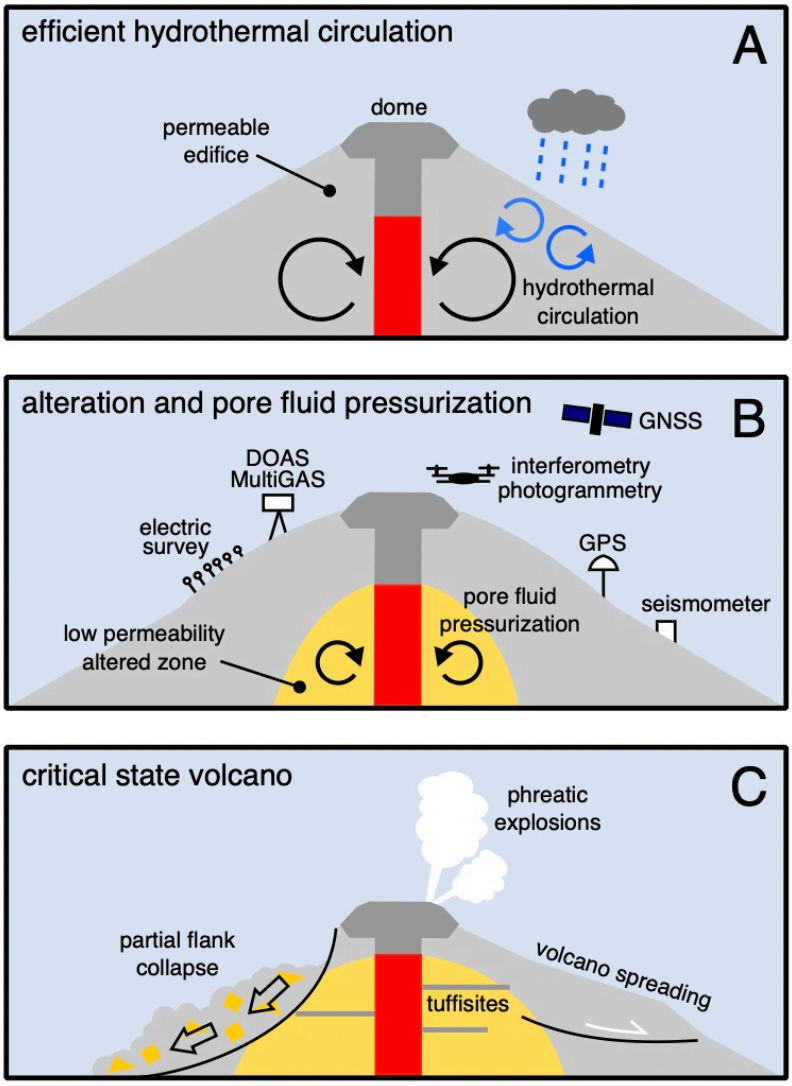

222

223 **Fig. 3.** A: Efficient hydrothermal circulation within a porous and permeable edifice. B:
224 Hydrothermal circulation creates an alteration zone with a lower permeability (yellow zone) that
225 results in pore fluid pressurization. “Geomojis” highlight some of the monitoring techniques. C:
226 Implications of a pressurized critical state volcano include: volcano spreading, partial flank
227 collapse, hydrofracturing/tuffisite formation, and phreatic/phreatomagmatic explosions.

REFERENCES CITED

Apuani, T., Corazzato, C., Cancelli, A., and Tibaldi, A., 2005, Physical and mechanical properties of rock masses at Stromboli: a dataset for volcano instability evaluation. Bulletin of Engineering Geology and the Environment, v. 64(4), p. 419-431.

Ball, J. L., Taron, J., Reid, M. E., Hurwitz, S., Finn, C., and Bedrosian, P., 2018, Combining multiphase groundwater flow and slope stability models to assess stratovolcano flank collapse in the Cascade Range. Journal of Geophysical Research: Solid Earth, v. 123(4), p. 2787-2805.

Bauville, A., and Baumann, T. S., 2019, geomIO: An Open-Source MATLAB Toolbox to Create the Initial Configuration of 2-D/3-D Thermo-Mechanical Simulations From 2-D Vector Drawings. Geochemistry, Geophysics, Geosystems, v. 20(3), p. 1665-1675.

Cecchi, E., van Wyk de Vries, B., and Lavest, J. M., 2004, Flank spreading and collapse of weak-cored volcanoes. Bulletin of Volcanology, v. 67(1), p. 72-91.

Clynne, M. A., and Muffler, L. P., 2017, Geologic field-trip guide to the Lassen segment of the Cascades Arc, northern California (No. 2017-5022-K2). US Geological Survey.

Day, S. J., 1996, Hydrothermal pore fluid pressure and the stability of porous, permeable volcanoes. Geological Society, London, Special Publications, v. 110(1), p. 77-93.

del Potro, R., and Hürlimann, M., 2009, The decrease in the shear strength of volcanic materials with argillic hydrothermal alteration, insights from the summit region of Teide stratovolcano, Tenerife. Engineering Geology, v. 104(1-2), p. 135-143.

de Moor, J. M., Stix, J., Avard, G., Muller, C., Corrales, E., Diaz, J. A., Alan, A., Brenes, J., Pacheco, J., Aiuppa, A., and Fischer, T. P., 2019, Insights on hydrothermal-magmatic

interactions and eruptive processes at Poás Volcano (Costa Rica) from high-frequency gas monitoring and drone measurements. Geophysical Research Letters, v. 46(3), p. 1293-1302.

Farquharson, J. I., Wild, B., Kushnir, A. R., Heap, M. J., Baud, P., and Kennedy, B., 2019, Acid-induced dissolution of andesite: evolution of permeability and strength. Journal of Geophysical Research: Solid Earth, v. 124(1), p. 257-273.

Finn, C. A., Deszcz-Pan, M., Anderson, E. D., and John, D. A., 2007, Three-dimensional geophysical mapping of rock alteration and water content at Mount Adams, Washington: Implications for lahar hazards. Journal of Geophysical Research: Solid Earth, v. 112(B10).

Frolova, F., Ladygin, V., Rychagov, S., & Zukhubaya, D., 2014, Effects of hydrothermal alterations on physical and mechanical properties of rocks in the Kuril–Kamchatka island arc. Engineering Geology, v. 183, p. 80-95.

Harlow, F. H., and Welch, J. E., 1965, Numerical calculation of time-dependent viscous incompressible flow of fluid with free surface. The Physics of Fluids, v. 8(12), p. 2182-2189.

Heap, M. J., and Violay, M.E.S., 2021, The mechanical behaviour and failure modes of volcanic rocks: A review. Bulletin of Volcanology, doi: 10.1007/s00445-021-01447-2.

Heap, M. J., Troll, V. R., Kushnir, A. R., Gilg, H. A., Collinson, A. S., Deegan, F. M., Darmawan, H., Seraphine, N., Neuberg, J., and Walter, T. R., 2019, Hydrothermal alteration of andesitic lava domes can lead to explosive volcanic behaviour. Nature Communications, v. 10(1), p. 1-10.

Heap, M. J., Gravley, D. M., Kennedy, B. M., Gilg, H. A., Bertolett, E., and Barker, S. L., 2020a, Quantifying the role of hydrothermal alteration in creating geothermal and epithermal mineral resources: the Ohakuri ignimbrite (Taupō Volcanic Zone, New Zealand). Journal of Volcanology and Geothermal Research, v. 390, 106703.

Heap, M. J., Villeneuve, M., Albino, F., Farquharson, J. I., Brothelande, E., Amelung, F., Got, J.-L., and Baud, P., 2020b, Towards more realistic values of elastic moduli for volcano modelling. Journal of Volcanology and Geothermal Research, v. 390, 106684.

Hoek, E., Carranza-Torres, C., and Corkum, B., 2002, Hoek-Brown failure criterion-2002 edition. Proceedings of NARMS-Tac, v. 1(1), p. 267-273.

John, D. A., Sisson, T. W., Breit, G. N., Rye, R. O., and Vallance, J. W., 2008, Characteristics, extent and origin of hydrothermal alteration at Mount Rainier Volcano, Cascades Arc, USA: Implications for debris-flow hazards and mineral deposits. Journal of Volcanology and Geothermal Research, v. 175(3), p. 289-314.

Kaus, B., Popov, A. A., Baumann, T., Pusok, A., Bauville, A., Fernandez, N., and Collignon, M., 2016, Forward and inverse modelling of lithospheric deformation on geological timescales. In: Proceedings of NIC Symposium (Eds: Binder, K., Müller, M., Kremer, M., Schnurpfeil, A.), John von Neumann Institute for Computing (NIC), NIC Series, v. 48, ISBN 978-3-95806-109-5.

Kereszturi, G., Schaefer, L. N., Miller, C., and Mead, S., 2020, Hydrothermal Alteration on Composite Volcanoes: Mineralogy, Hyperspectral Imaging, and Aeromagnetic Study of Mt Ruapehu, New Zealand. Geochemistry, Geophysics, Geosystems, v. 21(9), e2020GC009270.

Kennedy, B. M., Farquhar, A., Hilderman, R., Villeneuve, M. C., Heap, M. J., Mordensky, S., Kilgour, G., Jolly, A., Christenson, B., and Reuschlé, T., 2020, Pressure controlled permeability in a conduit filled with fractured hydrothermal breccia reconstructed from ballistics from Whakaari (White Island), New Zealand. Geosciences, v 10(4), 138.

López, D. L., and Williams, S. N., 1993, Catastrophic volcanic collapse: relation to hydrothermal processes. Science, v. 260(5115), p. 1794-1796.

Mordensky, S. P., Villeneuve, M. C., Kennedy, B. M., Heap, M. J., Gravley, D. M., Farquharson, J. I., and Reuschlé, T., 2018, Physical and mechanical property relationships of a shallow intrusion and volcanic host rock, Pinnacle Ridge, Mt. Ruapehu, New Zealand. Journal of Volcanology and Geothermal Research, v. 359, p. 1-20.

Moretti, R., Komorowski, J. C., Ucciani, G., Moune, S., Jessop, D., de Chabalier, J. B., Beauducel, F., Bonifacie, M., Burtin, A., Vallée, M., Deroussi, S., Robert, V., Gibert, D., Didier, T., Kitou, T., Feuillet, N., Allard, P., Tamburello, G., Shreve, T., Saurel, J.-M., Lemarchand, A., Rosas-Carbajal, M., Agrinier, P., Le Friant, A., and Chaussidon, M., 2020, The 2018 unrest phase at La Soufrière of Guadeloupe (French West Indies) andesitic volcano: Scrutiny of a failed but prodromal phreatic eruption. Journal of Volcanology and Geothermal Research, v. 393, 106769.

Reid, M. E., Sisson, T. W., and Brien, D. L., 2001, Volcano collapse promoted by hydrothermal alteration and edifice shape, Mount Rainier, Washington. Geology, v. 29(9), p. 779-782.

Reid, M. E., 2004, Massive collapse of volcano edifices triggered by hydrothermal pressurization. Geology, v. 32(5), p. 373-376.

Rosas-Carbajal, M., Komorowski, J. C., Nicollin, F., and Gibert, D, 2016, Volcano electrical tomography unveils edifice collapse hazard linked to hydrothermal system structure and dynamics. Scientific Reports, v. 6, 29899.

Rosas-Carbajal, M., Jourde, K., Marteau, J., Deroussi, S., Komorowski, J. C., and Gibert, D., 2017, Three-dimensional density structure of La Soufrière de Guadeloupe lava dome from

simultaneous muon radiographies and gravity data. Geophysical Research Letters, v. 44(13), p. 6743-6751.

van Wyk de Vries, B., and Francis, P. W., 1997, Catastrophic collapse at stratovolcanoes induced by gradual volcano spreading. Nature, v. 387(6631), p. 387-390.

van Wyk de Vries, B., Kerle, N., and Petley, D., 2000, Sector collapse forming at Casita volcano, Nicaragua. Geology, v. 28(2), p. 167-170.

Wyering, L. D., Villeneuve, M. C., Wallis, I. C., Siratovich, P. A., Kennedy, B. M., Gravley, D. M., & Cant, J. L., 2014, Mechanical and physical properties of hydrothermally altered rocks, Taupo Volcanic Zone, New Zealand. Journal of Volcanology and Geothermal Research, v. 288, p. 76-93.

[1]GSA Data Repository item 202Xxxx, containing a sample location maps and photographs, sample photographs, thin section images, the mineral componentry of the samples, additional methods, the presentation of some of the laboratory data, more details on the upscaling and model, and additional models is available online at www.geosociety.org/pubs/ft20XX.htm, or on request from editing@geosociety.org.